Calculation of Stresses in Stiffened Composite Panels

M. W. Hyer* and David Cohen†
Virginia Polytechnic Institute and State University, Blacksburg, Virginia

A methodology for computing the stresses at the interface between the skin and stiffener in stiffened composite panels is described. The methodology is based on finite-element analyses and an elasticity solution. The finite-element analyses are standard, while the elasticity solution is based on eigenvalue expansions of the stress functions. The eigenvalue expansions are assumed to be valid in the local region where the stiffener flange terminates. The local elasticity solution is coupled to the global finite-element analysis using collocation on the boundary of the local region. Accuracy and convergence of the method are discussed and several examples of its utility are presented.

Introduction

THE purpose of this paper is to describe a methodology that is being developed to investigate the state of stress that exists at the interface between a composite skin and the flanges of a cocured or secondarily bonded composite stiffener. As will be seen, the idea can be extended to a variety of other situations, but emphasis here is on the skin-stiffener problem. Once developed, this methodology will be used to study the influence of the structural, geometric, and material parameters on the interface stresses. More importantly, it will be used to design against failure of the structure at the skin-stiffener interface. The approach here is more rigorous than existing approaches used to study this class of problems (e.g., See Ref. 1) and relies on three levels of analysis, herein referred to as structural, global, and local levels. The subject of this paper is primarily the latter level, though the global level is discussed somewhat. The analysis at the local level is based on an elasticity approach to computing the stresses. In particular, the local analysis is based on an eigenvalue expansion of the stress functions that govern the stresses in the interface region, specifically the region where the flange terminates. The eigenvalue expansion approach was used by Wang and Choi,[2] Ting and Chou,[3] and Delale[4] in the study of stresses at the free edges of composite laminates. Portions of the methodology described here are based on these works. The development of the methodology is multistepped and consists of 1) development for linear structural analysis; 2) application to the study of interface stresses for linear structural problems; 3) extension to include geometric nonlinearities in the analysis; and 4) application to the study of interface stresses for geometrically nonlinear problems. In all of the work the material behavior is assumed to be linear elastic to failure. This paper is a summary of work in the first two steps. Discussions of the other steps will appear in subsequent papers.

Overview of Problem and Methodology

The specific problem being studied is depicted in Fig. 1, which shows a composite skin stiffened with a T-type stiffener, the horizontal portion of the T acting as a flange and being bonded to the skin. It is assumed that the bond between the flange and skin is perfect and the bondline is of zero thickness. At this point, neither the loading on the panel nor the particular boundary conditions along the edges of the panel are important. However, an analysis of the stiffened panel with prescribed boundary and loading conditions constitutes what is referred to as the structural-level analysis. The result of such an analysis is the stress resultants at any point in the structure. Although other structural responses are calculated as a result of such an analysis, only the stress resultants are of interest.

The coordinate system used in the analysis is shown in Fig. 1; z describing the longitudinal location along the panel and the x and y describing the transverse cross-sectional location. Attention will be focused on a cross section of the panel. An important assumption in the analysis is as follows: the cross section being considered is taken at a longitudinal location along the panel such that the stress state is not a function of the longitudinal coordinate z. The analysis is confined to the region away from the ends of the panel where clamped, simple-support, or other conditions strongly influence the stress state. This independence of the stresses, and hence strains, of the z coordinate categorizes the problem as one of generalized plane deformation.[5]

Figure 2 shows the details of a transverse cross section, particularly the flange termination region. In reality, only one-half the cross section shown is analyzed because, despite the errors incurred in certain situations (e.g., see Ref. 6), the analysis here is assumed to be of a symmetric problem. The analysis of the cross section shown in Fig. 2 is what is referred to here as the global-level analysis. The analysis of the flange-termination region, the inset, is what is referred to as the local-level analysis. The stress resultants N, Q, and M shown at the left and right ends of the cross section are determined from the structural-level analysis. Also to be specified from the structural-level analysis are the stress resultants acting on the cross section of Fig. 2, e.g., N_z. Alternatively, the deformations in the z direction, e.g., curvature in the z direction, can be specified.

The global-level analysis, like the structural-level analysis, is accomplished with finite elements and, at least for the linear problems, is quite straightforward. The local-level analysis is assumed to be valid in the flange termination region. The boundary conditions for the local analysis are provided by the global analysis. The boundary of the local region, shown in Fig. 2 for this problem as BCDEF, is chosen to be far enough away from the actual flange termination point, point A, so that the global analysis of the stresses on the boundary of the local region is unaffected by the termination geometry. Attention now turns to discussing the analysis of this local region.

Received Jan. 13, 1987; presented as Paper 87-0731 at the 28th AIAA Structures, Structural Dynamics, and Materials Conference, Monterey, CA, April 6-8, 1987; revision received Dec. 24, 1987.

*Professor, Department of Engineering Science and Mechanics. Associate Fellow AIAA.

†Graduate Student, Department of Engineering Science and Mechanics; currently, Hercules, Inc., Magna, UT. Member AIAA.

Local Analysis

The local region is considered to be dominated by the fact that the flange terminates at a known angle β relative to the skin. The flange and skin can be made of different materials and, as mentioned previously, are perfectly bonded together with a bondline of zero thickness. The material properties of the flange and the skin are each assumed to be orthotropic. Although the flange and skin are made of multiple laminae of fiber-reinforced material, in each case the effects of the multiple laminae are smeared to obtain equivalent orthotropic material properties. These properties are assumed to be valid through the thickness of the flange and skin. Essentially with this smearing it is assumed that the details of the interaction between the skin and flange are governed by the overall material properties of these two subcomponents, rather than by the material properties of the top lamina of the skin that is bonded to the bottom lamina of the flange. In this study, the flange termination region is cast in such a way that the flange termination region is a special case of a bimaterial wedge. As is done in those studies, the wedge is analyzed as if it were a semi-infinite domain. This can be visualized by allowing points B, C, D, E, and F in the inset of Fig. 2 to move to infinity in the various directions. The results of the analysis of the semi-infinite domain are then actually applied over the finite region bounded by BCDEF of Fig. 2. The boundary conditions on AB and FA are satisfied exactly while the boundary conditions on the remainder of the contour are made to match, in a least-squares sense, the contour conditions as calculated by the global analysis.

Considering semi-infinite wedges, the conditions that must be enforced on the boundary and at the interface between the two materials are

$$\sigma_\theta^{(1)}(r, \beta) = \tau_{r\theta}^{(1)}(r, \beta) = \tau_{z\theta}^{(1)}(r, \beta) = 0$$

$$\sigma_\theta^{(2)}(r, -\pi) = \tau_{r\theta}^{(2)}(r, -\pi) = \tau_{z\theta}^{(2)}(r, -\pi) = 0$$

$$\sigma_\theta^{(1)}(r, 0) = \sigma_\theta^{(2)}(r, 0)$$

$$\tau_{r\theta}^{(1)}(r, 0) = \tau_{r\theta}^{(2)}(r, 0)$$

$$\tau_{z\theta}^{(1)}(r, 0) = \tau_{z\theta}^{(2)}(r, 0)$$

$$u^{(1)}(r, 0, z) = u^{(2)}(r, 0, z)$$

$$v^{(1)}(r, 0, z) = v^{(2)}(r, 0, z)$$

$$w^{(1)}(r, 0, z) = w^{(2)}(r, 0, z) \tag{1}$$

The superscripts in Eq. (1) represent the material number; 1 denoting the flange, 2 denoting the skin. Note that polar notation is being used and the origin of the coordinate system is located at the vertex of the wedge, point A in Fig. 2. Conventional notation is being used for the stresses, and u, v, and w represent displacements in the radial, circumferential, and z directions, respectively. To analyze this bimaterial wedge region, subjected to the above conditions, the method of complex potentials, in conjunction with the concept of an eigenvalue expansion,[2] is used. That work is briefly summarized here as it applied to this problem.

Bearing in mind that the stresses are independent of z, the equilibrium equations, in Cartesian coordinates, for the local region become

$$\frac{\partial \sigma_x}{\partial x} + \frac{\partial \tau_{xy}}{\partial y} = 0$$

$$\frac{\partial \tau_{xy}}{\partial x} + \frac{\partial \sigma_y}{\sigma y} = 0$$

$$\frac{\partial \tau_{xz}}{\partial x} + \frac{\partial \tau_{yz}}{\partial y} = 0 \tag{2}$$

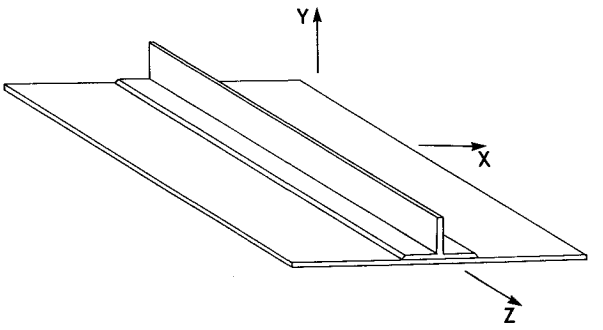

Fig. 1 Overall configuration of stiffened panel.

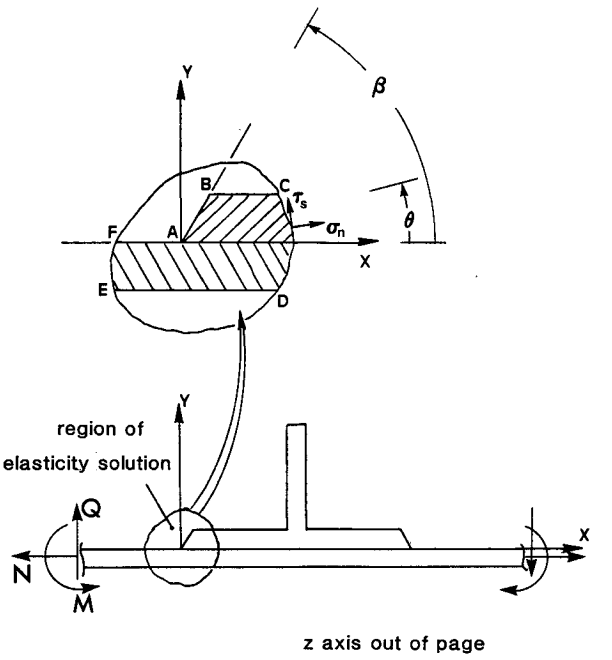

Fig. 2 Skin-stiffener cross-sectional geometry.

Defining a pair of stress functions, F and ψ, the equilibrium equations are automatically satisfied if the stresses are related to the stress functions by

$$\sigma_x = \frac{\partial^2 F}{\partial y^2}, \qquad \sigma_y = \frac{\partial^2 F}{\partial x^2}, \qquad \tau_{xy} = -\frac{\partial^2 F}{\partial x \partial y}$$

$$\tau_{yz} = -\frac{\partial \psi}{\partial x}, \qquad \tau_{xz} = \frac{\partial \psi}{\partial y} \tag{3}$$

It should be noted that there is a pair of stress functions for the flange and a pair for the skin. Using the constitutive relation and the fact that the stresses and strains are independent of the z coordinate, the strain-displacement relations can be integrated to obtain expressions for the three components of displacement. These integrated expressions are

$$u = -\frac{B_1 a_{33}}{2} z^2 - B_4 yz + U(x,y) + \omega_2 z - \omega_3 y + u_0$$

$$v = -\frac{B_2 a_{33}}{2} z^2 + B_4 xz + V(x,y) + \omega_3 z - \omega_1 z + v_0$$

$$w = (B_1 x + B_2 y + B_3) a_{33} z + W(x,y) + \omega_1 y - \omega_2 x + \omega_0 \tag{4}$$

In arriving at these expressions, the constitutive behavior is assumed to be of the form

$$\begin{Bmatrix} \epsilon_x \\ \epsilon_y \\ \epsilon_z \\ \gamma_{yz} \\ \gamma_{xz} \\ \gamma_{xy} \end{Bmatrix} = \begin{bmatrix} a_{11} & a_{12} & a_{13} & 0 & 0 & 0 \\ a_{12} & a_{22} & a_{23} & 0 & 0 & 0 \\ a_{13} & a_{23} & a_{33} & 0 & 0 & 0 \\ 0 & 0 & 0 & a_{44} & 0 & 0 \\ 0 & 0 & 0 & 0 & a_{55} & 0 \\ 0 & 0 & 0 & 0 & 0 & a_{66} \end{bmatrix} \begin{Bmatrix} \sigma_x \\ \sigma_y \\ \sigma_z \\ \tau_{yz} \\ \tau_{xz} \\ \tau_{xy} \end{Bmatrix} \tag{5}$$

and the standard strain-displacements relations in Cartesian coordinates are integrated. In the constitutive relations, the a_{ij} are the smeared components of the compliance matrix. In Eq. (4), u, v, and w are now the displacements in the x, y, and z directions, and U, V, and W are arbitrary functions. The remaining terms are constants of integration. The arbitrary functions U, V, and W must satisfy the relations

$$\frac{\partial U}{\partial x} = \beta_{11}\sigma_x + \beta_{12}\sigma_y + a_{13}(B_1 x + B_2 y + B_3)$$

$$\frac{\partial V}{\partial y} = \beta_{21}\sigma_x + \beta_{22}\sigma_y + a_{23}(B_1 x + B_2 y + B_3)$$

$$\frac{\partial U}{\partial y} + \frac{\partial V}{\partial x} = \beta_{66}\tau_{xy}$$

$$\frac{\partial W}{\partial x} = \beta_{55}\tau_{xz} + B_4 y$$

$$\frac{\partial W}{\partial y} = \beta_{44}\tau_{yz} - B_4 x \tag{6}$$

where β_{ij} are the reduced compliances and are given by

$$\beta_{ij} = a_{ij} - \frac{a_{i3}a_{j3}}{a_{33}}, \qquad i = 1,2,4,5,6 \tag{7}$$

The equations governing F and ψ are derived by writing the right-hand sides of Eq. (6) in terms of the stress functions and elimination U, V, and W from these equations by differentiation. These equations are

$$\beta_{22}\frac{\partial^4 F}{\partial x^4} + (2\beta_{12} + \beta_{66})\frac{\partial^4 F}{\partial x^2 \partial y^2} + \beta_{11}\frac{\partial^4 F}{\partial y^4} = 0$$

$$\beta_{44}\frac{\partial^2 \psi}{\partial x^2} + \beta_{55}\frac{\partial^2 \psi}{\partial y^2} = -2B_4 \tag{8}$$

The stress functions satisfying the homogeneous portion of Eq. (8) are approximated by series with terms of the form

$$F(Z) = C\frac{Z^{\lambda+2}}{(\lambda+1)(\lambda+2)}$$

$$\psi(\tilde{Z}) = D\frac{\tilde{Z}^{\delta+1}}{(\delta+1)} \tag{9}$$

where the complex variables Z and $\tilde{Z}$ are defined by

$$Z = x + \mu y$$

$$\tilde{Z} = x + \nu y \tag{10}$$

μ and ν being known material constants, and C and D are to-be-determined constants. The exponents λ and δ are also to be determined. Substitution of Eq. (9) into the homogeneous part of Eq. (8) leads to

$$C\lambda(\lambda-1)Z^{\lambda-2}[\beta_{22} + (2\beta_{12} + \beta_{66})\mu^2 + \beta_{11}\mu^4] = 0$$

$$D\delta\tilde{Z}^{\delta-1}[\beta_{44} + \beta_{55}\nu^2] = 0 \tag{11}$$

The first of Eq. (11) is satisfied if $\lambda = 0$ or 1, or if the expression in square brackets is zero. Four distinct values of μ make the bracketed term zero. As a result, F has the form

$$F(x,y) = \sum_{k=1}^{4} C_k \frac{Z_k^{\lambda+2}}{(\lambda+1)(\lambda+1)} + b_1 x^3 + b_2 x^2 y + b_3 x y^2 + b_4 y^3 + b_5 x^2 + b_6 x y + b_7 y^2 \tag{12}$$

where the polynomial in x and y corresponds to the conditions $\lambda = 0,1$; the summation accounts for the four values of μ; and $Z_k = x + \mu_k y$, $k = 1,4$. The b_i in Eq. (12) are to-be-determined constants. Similarly, the second of Eq. (11) is zero if $\delta = 0$, or if the expression in square brackets is zero. The latter condition is satisfied by two values of ν. As a final result, ψ has the form

$$\psi(x,y) = \sum_{k=1}^{2} D_k \frac{\tilde{Z}_k^{\delta+1}}{(\delta+1)} + b_8 x + b_9 y + b_{10} x^2 + b_{11} y^2 \tag{13}$$

where $\tilde{Z}_k = x + \nu_k y$, $k = 1,2$. The last two terms in Eq. (13) represent the particular solution for ψ.

As a result of the above development, the six components of stress and the three components of displacement in the local region are written in terms of the expressions in Eqs. (12) and (13). The displacement expressions result when the stresses are substituted into Eq. (6), and those relations are integrated for U, V, and W, Eq. (4) then being used. The expressions for the stresses and displacements are converted to polar notation and substituted into Eq. (1) to enforce the boundary and interface conditions of the local region. Because of the assumed orthotropic nature of both the skin and flange, enforcement of Eq. (1) leads to two separate and uncoupled eigenvalue problems. One problem involves u, v, σ_x, σ_y, τ_{xy} and the other involves w, τ_{xz}, and τ_{yz}. The former is referred to as the inplane problem whereas the latter is referred to as the out-of-plane problem. The inplane problem involves λ as eigenvalues and the constants C, and the out-of-plane problem involves δ as eigenvalues and the constants D. The eigenvalues λ are, in general, complex, whereas the eigenvalues δ are real. Finding the δ is straightforward. Finding the λ is not straightforward and is a key step in the methodology. There are an infinite number of both λ and δ that satisfy Eq. (1) but only those that lead to bounded displacements are of physical significance. To have bounded displacements, the real part of the eigenvalue must be greater than -1. Even with this restraint, the stresses may be unbounded, leading to a severe stress gradient in the local region. Physically, this might be expected and the methodology shows that this can indeed be the case. For this class of problems, it appears that only the λ lead to unbounded stresses and the δ lead to bounded stresses. In addition, it can be shown that with no twisting of the plate about the z axis, with orthotropic materials there are no out-of-plane stresses τ_{xz} and τ_{yz}. Therefore, for the remainder of this discussion, only the inplane problem will be discussed.

With each eigenvalue λ and associated eigenvector, the eigenvector relating the four constants C_k of the series in Eq. (12), there is one undetermined coefficient c_m. Considering M eigenvalues, the expression for F is actually a double series of the form

$$\sum_{m=1}^{M} c_m \left(\sum_{k=1}^{4} \phi_m^k \frac{Z_k^{\lambda_m+2}}{(\lambda_m+1)(\lambda_m+2)} \right) \tag{14}$$

where the ϕ_m^k represent the components of the eigenvector associated with the mth eigenvalue, and c_m are the undetermined coefficients. The values of the c_m are determined by using stresses from the global analysis of the cross section. The global analysis provides accurate values of the stresses on the boundary of the local region, provided the mesh used in the finite-element analysis is not too coarse and the contour is a sufficient distance from point A. Clearly the terms "not too

coarse" and "sufficient distance" are, at this point, ambiguous and must be clearly defined. However, assuming that the stresses on the contour are known from the global analysis, then the stresses from the elasticity solution can be made to match these stresses by the proper choice of the c_m. There are a variety of ways to do this and the method used here is discussed next.

Collocation Procedure

From the global analysis, the normal and shear stresses σ_n and τ_s (see inset of Fig. 2) at a number of points on the contour are determined. As depicted in the inset of Fig. 2, the contour for the specific problem here actually includes the upper and lower surfaces of the flange-skin cross section, lines BC and DE. For the problems to be discussed below, σ_n and τ_s are exactly zero on BC and DE. Thus, the global analysis is used to provide the stresses only on portions CD and EF of the contour. If the response to a pressure on the top and/or bottom surface of the panel is being studied, portions of the contour, namely, portions FABC and/or DE, are not traction free. However, compared to the stresses generated as a result of this pressure, the pressure condition on the boundary is very small and can be ignored.

With the values of σ_n and τ_s known at a specific number of points along contour BCDEF, the values of c_m in a series with almost twice as many eigenvalues as there are points can be determined uniquely by equating the numerical values of the globally computed stresses at these points to the stresses expressed in terms of the c_m. In addition to the unknown c_m, some of the constants b_i in Eq. (12) must also be determined. Therefore the number of eigenvalues that can be used is slightly less than twice the number of points of the contour. Here, instead of using exactly the correct number of points on the contour, more are used. Then the error between the numerical value of the globally computed stresses at these points and the stresses at these points expressed in terms of c_m and b_i is minimized, in a least-squares sense, with respect to the c_m and b_i. The result is an overdetermined set of equations for computing the values of c_m and b_i. Such a scheme has been used in similar situations.[7]

With the values of c_m and b_i determined, the stresses at any point within the local region can be computed. The influence of the flange and skin material properties, the flange thickness, the flange termination angle, and other parameters on the stress state can be determined. The influence of these parameters on the stress eigenfactor, defined as[2]

$$K_i = \lim_{x \to 0} x^{-\lambda_1} \sigma_i(x, 0) \tag{15}$$

can also be studied. In the above, $\sigma_i = \sigma_x$, σ_y, or τ_{xy} and λ_1 is the eigenvalue that has its real part closest to -1. The stress eigenfactor measures the rate at which the stress becomes unbounded as the vertex in the flange termination region is approached. The concept has the advantage that one parameter can be used to quantify the severity of the stress state.

The discussion now turns to numerical results that describe the accuracy and convergence of this method. In this context, three important issues are addressed. First to be addressed is how accurately the stresses as predicted by the eigenvalue expansion represent the stresses within the local region. Second, the influence on the predicted stresses of the number of eigenvalues in the series is discussed. And third, the influence on the predicted stresses of the number of collocation points is considered. Other issues, alluded to earlier, related to the fineness of the mesh in the global analysis and the distance of the contour from the vertex of the flange termination, are addressed.

Numerical Results

The example used to discuss the accuracy and convergence of the method consists of a long stiffened panel with known moments applied along opposite longitudinal edges. The curvature and elongation in the z direction are taken to be zero. This loading is essentially that shown in Fig. 2 with the shear and inplane stress resultants, Q and N, removed. Such a loading, although perhaps of little physical significance, was chosen because it produces a significant peel and shear stresses between the flange and skin. In this example, the skin is orthotropic with a $(\pm 45/90_2)_s$ layup, and the flange is quasi-isotropic with a $(\pm 45/0/90)_s$ layup, the fiber direction being measured relative to the z axis of Fig. 1. The smeared flange and skin properties are given in Table 1. The flange determination angle β is 45 deg, and the flange is 25.4 mm wide. Figure 3 shows the finite-element discretization of the problem. Contour BCDEF and the applied moment are shown. As might be expected, the issues of the distance of the contour from the vertex and the fineness of the global analysis mesh are coupled and will be discussed first.

In a finite-element analysis of a layered solid, because of the difference in material properties in the layers, there is usually a set of elements on one side of the interface between the layers and another set of elements on the other side. For those stress components that are continuous across the interface (here σ_y and τ_{xy}), the stresses computed in the elements on one side of the interface should be equal to the stresses computed in the elements on the other side of the interface. If this is not the case, the finite-element representation is in error. This often happens in regions of rapidly changing stresses, indicating that the mesh is not refined enough. Here in Fig. 3, as the termination region is approached from the right, at a certain distance from the vertex (point A), the stresses from finite elements on either side of the interface do not agree. If the mesh is refined further, the point at which the stresses disagree moves closer to the vertex. With this in mind, it is clear that an important consideration is to have the contour dimensions large enough and the mesh fine enough so the contour passes through those elements that properly exhibit stress continuity. Many combinations of contours and mesh densities satisfying this criteria are possible. Here, to narrow the choices, the dimension of the contour is related to the characteristic dimension of the problem, namely, the thickness of the flange-skin combination $2t_s$. In this example, the skin thickness t_s and the flange thickness are the same, and so the total thickness is $2t_s$. Here the length of the contour (length BC in Fig. 3) is chosen to be $3t_s$.

To determine whether the eigenvalue expansion accurately represents the stresses in the localized region, the results of a sequence of finite-element analyses of the local region, using an increasingly finer mesh in the local region, are compared to the predictions of the eigenvalue analysis. Figure 4 illustrates the findings. The figure illustrates the shear stress τ_{xy} at the interface as predicted by the eigenvalue solution and as predicted by progressive refinements of the mesh. For the eigenvalue solution, 15 eigenvalues and 90 collocation points are used. As mentioned earlier, this component of stress is continuous across the interface. The horizontal axis in the

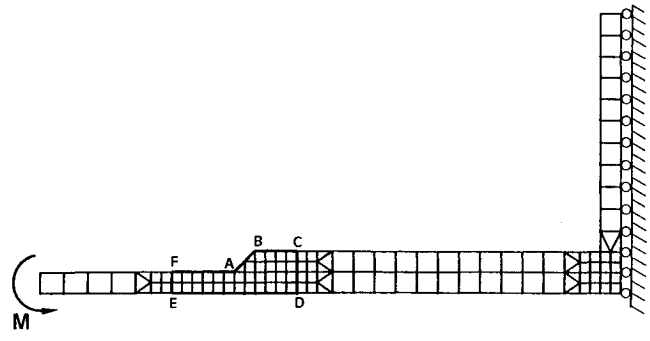

Fig. 3 Finite-element discretization of skin-stiffener cross section.

figure $\bar{x}$ is the distance from the vertex divided by the skin thickness, i.e., $\bar{x}=x/t_s$. The vertical axis $\bar{\tau}_{xy}$ is the shear stress normalized by the maximum value of the bending stress σ_x in the skin, away from the flange. For this problem, τ_{xy} is unbounded at the vertex, and so obviously the vertical axis is truncated. The refined mesh is twice as dense, in the local region, as the coarse mesh, and the fine mesh is twice again as dense. The finite-element predictions on both the skin and the flange side of the interface are shown. As can be seen from the three portions of the figure, as the mesh is refined, the shear stress prediction from the finite-element analysis exhibits a better and better degree of continuity. What is more important, the eigenvalue solution agrees very well with the stress state to which the finite-element solution appears to be converging. A similar characteristic was found for σ_y. Althought indirect, this approach to studying the accuracy of the eigenvalue solution is really the only one possible within the context of this problem. Furthermore, it illustrates the previously discussed point of requiring stress continuity. When looking at Fig. 4, the reader should be reminded that $\bar{x}=3$ is on the contour line CD. It should be mentioned also that the coarse, refined, and fine mesh give identical results for the numerical values of the stresses on the contour of the local region. Thus, only one coarse mesh is needed to compute the stresses on the contour.

The influence of the number of eigenvalues on the predicted stresses is illustrated in Fig. 5. Five, 10, and 15 eigenvalues and 90 collocation points are used to predict stresses in the local region, based on contour stresses computed from a coarse mesh. As can be seen, even five eigenvalues capture the important characteristics of the stress state in the local region. Doubling and tripling the number of terms in the series has little influence on the predicted stresses. Adding eigenvalues beyond five simply refines the predictions in selected areas. In fact, for this problem adding eigenvalues refines the predictions away from the vertex, the region where the local solution would be the least accurate when using a minimum number of eigenvalues. This characteristic of the solution is much like needing only a few modes to describe accurately the gross vibratory motion of a structure.

The influence of the number of collocation points on the predicted stresses is seen in Fig. 6. It is seen that halving the number of collocation points, from 90 to 45, has no influence on the predicted stress. It was found that as long as the number of collocation points is one and a half times the number of unknown coefficients, realizing c_m can constitute one or two unknowns depending on whether it is real or complex, the results are independent of the number of collocation points. In Fig. 6 the stresses were computed using 15 eigenvalues.

To summarize this section, there is every indication that the methodology gives accurate and reliable information on the stress state within the local region. In addition, a coarse global level mesh can be used to generate the information on the boundary of the local region. Although no structural-level analysis was conducted here, it is clear that mesh can also be coarse. As a result, this entire computation can be accomplished on relatively small-scale computers at minimal cost.

Before proceeding, a comment is in order. To couple the local elasticity analysis with the global analysis, equilibrium of the local region is enforced through the collocation procedure. Compatibility of the displacements between the global and local regions is not enforced. If it were enforced, in addition

Table 1 Material properties[a]

	E_x	E_y	E_z	G_{xy}	G_{xz}	G_{yz}	ν_{xy}	ν_{xz}	ν_{yz}
Flange	56	15	56	5.9	21	5.9	0.16	0.30	0.04
Skin	81	15	26	5.9	21	5.9	0.1	0.61	0.10

[a]E's and G's in GPa.

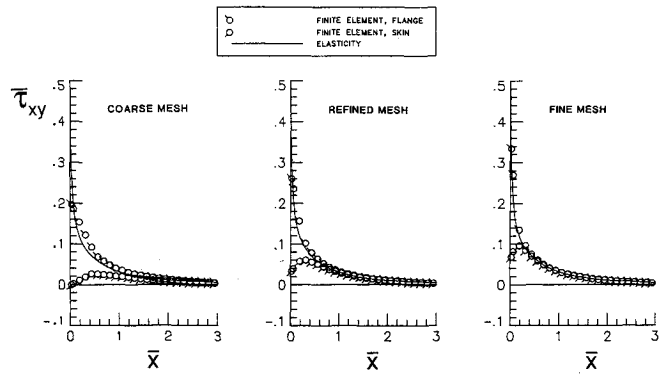

Fig. 4 Accuracy of stress calculations.

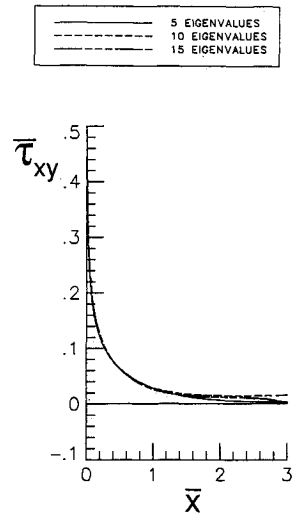

Fig. 5 Influence of the number of eigenvalues.

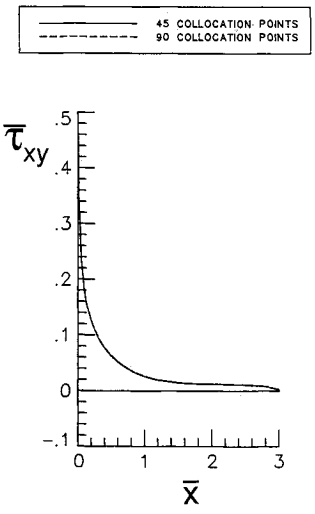

Fig. 6 Influence of the number of collocation points.

to enforcing equilibrium, a slight correction to the stresses that satisfy equilibrium would result, and through iteration, a set of displacements that satisfy compatibility could be found. It is felt here that the enforcement of either force equilibrium or compatibility is all that is required. Enforcement of force equilibrium seems to have advantages when the methodology is extended to geometrically nonlinear problems.

Additional Numerical Results

To illustrate the utility of the methodology, the influence on the stress state of changing the flange termination angle and of changing the flange thickness is investigated. Specifically, the effect of changing the flange termination angle to 90 deg and then also doubling the thickness of the flange is discussed. For variety, a different physical situation is discussed. For this portion of the discussion, the panel is given a known curvature in the z direction. There are no tractions acting on the longitudinal edges. Because of different elastic properties, the anticlastic curvature of the flange would be different than the anticlastic curvature of the skin and the flange and skin. If they were not bonded together, they would spread apart. Since they are bonded together, stresses develop. Table 2 presents the stress eigenfactors for the peel stress K_y and the shear stress K_{xy} generated as a result of the flange and skin being bonded together. To simplify the discussion, the factors have been normalized by K_y for the case of a 45 deg flange angle and the flange thickness equal to the skin thickness. The flange and skin being of equal thickness is referred to as the thin flange case.

Table 2 Stress Eigenfactors

	45 deg angle thin flange	90 deg angle thin flange	90 deg angle thick flange
K_y	1.0	3.2	3.6
K_{xy}	1.5	2.0	2.2

As can be seen from the table, for the case of a 45 deg flange termination angle and the thin flange, the shear stress eigenfactor is 1.5 times the magnitude of the peel stress eigenfactor. This indicates that the flange would be expected to separate from the skin with shear stresses dominating. Changing the flange termination angle to an abrupt 90 deg increases both the peel and shear factors. Relative to their respective values for the 45 deg angle case, the peel factor more than triples while the shear factor increases by 30%. This change in the flange termination angle to 90 deg causes the peel factor to be more important than the shear factor. This indicates that failure would be due to peel stresses dominating. Leaving the termination angle of the flange at 90 deg and doubling the flange thickness causes both stress eigenfactors to increase by only about 10% above the thin 90 deg case. This value is much smaller than expected. From intuition, these effects of changing the flange termination angle and thickness are to be expected. However, the methodology presented quantifies these effects and provides a direct measure of a change in a structural parameter on skin-stiffener interaction.

Before closing, another important point needs to be made. To study the influence of the flange termination angle, only one global finite-element analysis was needed. Had a structural-level analysis been involved, only one analysis at that level would have been required. Contour lines CD and EF were chosen to be far enough away from point A that the stresses on these lines were the same for the 90 deg flange angle case as for the 45 deg case. Hence, the eigenvalue solution for the 90 deg angle case was computed using the same set of global stresses as was used for the 45 deg case. The difference in the responses of the two cases comes only from the difference in the eigenvalues and associated eigenvectors. The influence of a 30 deg or 60 deg flange angle can be made with no further finite-element analyses. It is only necessary to recompute the results of the collocation scheme using the eigensolution for the desired flange angle. Although the structural and possibly the global levels of analysis may require moderate levels of computing, those analyses may only have to be conducted once and the results transferred to a smaller system where parameter studies using different local solutions can be made. This is a significant computational advantage.

Acknowledgments

The work presented here was supported through Grant NAG 1-343 with the Structural Mechanics Branch of the NASA Langley Research Center and is gratefully acknowledged. Dr. J. H. Starnes and Dr. M. P. Nemeth monitored the work, and their comments are appreciated.

References

[1]Wang, J. T. S. and Biggers, S. B., "Skin/Stiffener Interface Stresses in Composite Stiffened Panels," NASA CR 172261, 1984.

[2]Wang, S. S. and Choi, I., "Boundary-Layer Effects in Composite Laminates," Pt. 1 and Pt. 2., *Journal of Applied Mechanics,* Vol. 49, No. 3, Sept. 1982, pp. 541-560.

[3]Ting, T. C. T. and Chou, S. C., "Edge Singularities in Anisotropic Composites," *International Journal of Solids and Structures,* Vol. 17, No. 11, 1982, pp. 1057-1068.

[4]Delale, F., "Stress Singularities in Bonded Anisotropic Materials," *International Journal of Solids and Structures,* Vol. 20, No. 1, 1984, pp. 31-40.

[5]Lekhnitskii, S. G., *Theory of Elasticity of an Anisotropic Body,* Holden-Day, San Francisco, CA, 1963.

[6]Nemeth, M. P., "Importance of Anisotropic Bending Stiffness on Buckling of Symmetrically Laminated Composite Plates Loaded in Compression," *AIAA Journal,* Vol. 24, Nov. 1986, pp. 1831-35..

[7]Carpenter, W. C., "The Eigenvector Solution for General Corner of Finite Opening Crack with Further Studies on the Collocation Procedure," *International Journal of Fracture,* Vol. 27, No. 1, Jan. 1985, pp. 63-73.